JOURNAL OF GUIDANCE, CONTROL, AND DYNAMICS
Vol. 33, No. 2, March–April 2010

Periodic Orbits of Nonlinear Relative Dynamics Along an Eccentric Orbit

Mai Bando*
Kyoto University, Kyoto 611-0011, Japan
and
Akira Ichikawa†
Kyoto University, Kyoto 606-8501, Japan

DOI: 10.2514/1.46024

This paper is concerned with formation acquisition and reconfiguration problems with an eccentric reference orbit. As a first step, the characterization problem is considered for all initial conditions that constitute periodic solutions of the nonlinear equations of relative motion. Under the condition that the inertial orbits of the leader and a follower are coplanar, initial conditions of all periodic relative orbits are generated in terms of parameters of their orbits and their initial positions. Then the inertial orbit of the follower is rotated successively around the two axes of its perifocal reference system, and the initial conditions of all noncoplanar relative orbits are derived. Based on these periodic relative orbits, formation acquisition and reconfiguration problems by a feedback controller are formulated. The main performance index of a feedback controller is the total velocity change during the operation. Using the property of null controllability with vanishing energy of the Tschauner–Hempel equations, suboptimal controllers are designed via the differential Riccati equation of the linear regulator theory of periodic systems.

I. Introduction

EQUATIONS of relative motion with a circular reference orbit are nonlinear autonomous differential equations. The linearized equations around the null solution were introduced to study rendezvous problems [1]. Now they are known as Hill–Clohessy–Wiltshire (HCW) equations [2–4]. After the introduction of formation flying in the 1980s, the HCW equations were used for formationkeeping problems [5–8] and formation problems [9–16].

Vassar and Sherwood [5] assumed impulse maneuvers at given sampling times and employed the discrete-time linear quadratic regulator (LQR) theory. Leonard et al. [6] used three-valued differential drag between two satellites for controlling the relative motion. Redding et al. [7] proposed a controller based on feedforward control and the discrete-time LQR theory. Motivated by new developments in propulsion technologies, Kapila et al. [8] employed pulse control and designed stabilizing feedback controls by the discrete-time LQR theory.

Kong et al. [9] proposed formation flying for aperture synthesis with application to an Earth imager system. The HCW equations possess periodic solutions, and they are often used for formation problems. Kang et al. [10] used feedback linearization and the continuous-time LQR theory to track a periodic solution of the HCW equations. Campbell [11] considered a reconfiguration problem between two periodic solutions and formulated a minimum-time problem as well as a minimum-fuel problem, in which the time interval is finite and the cost function is the absolute integral of the thrust. Schaub [12] derived a description of the relative orbit in terms of orbit element differences for both circular and eccentric reference orbits. Vaddi et al. [13] considered formation and reconfiguration problems using orbit element differences and obtained a two-impulse solution. Palmer [14] considered a finite-time formation problem in which the square integral of the thrust accelerations is minimized and analytic solutions for the thrust functions are given. Shibata and Ichikawa [15] considered a formation reconfiguration problem by feedback for both circular and eccentric reference orbits. Ichimura and Ichikawa [16] considered a formation reconfiguration problem by impulse control. Designed feedback controllers in [10,15,16] were applied to the original nonlinear equations of relative motion, but periodic orbits used for formation flying were not their solutions. A more natural formation problem is to use periodic solutions of the nonlinear relative dynamics. Motivated by this observation, initial conditions of all periodic solutions of nonlinear equations of relative motion with a circular reference orbit have been explicitly given by Bando and Ichikawa [17] in terms of the initial true anomaly, mean motion, semimajor axis, and eccentricity of the follower's inertial orbit and its two rotation angles. A new formation problem has been solved using the linear regulator theory and the null controllability with vanishing energy (NCVE) of the HCW system [15].

Equations of relative motion with an eccentric reference orbit are nonlinear differential equations involving the radius and true anomaly of the eccentric orbit. The linearized equations around the null solution are also introduced to study rendezvous problems and are now known as Tschauner–Hempel (TH) equations [18–20]. The TH equations also have periodic solutions, which are useful for formation problems. They were characterized by Inalhan et al. [21], and the initialization procedure to periodic motion was given. Periodic solutions also follow from the transition matrix of the TH system in [22]. The effects of eccentricity on the shape and size of relative orbits were studied in [23]. The reconfiguration problem based on these periodic solutions was studied by Shibata and Ichikawa [15], and feedback controllers were designed using a differential Riccati equation and the NCVE property of the TH system. The main performance index is the L_1-norm of the control input. Periodic relative orbits of the TH equations are not solutions of the original nonlinear relative dynamics. Hence, if one considers a formation acquisition problem or a reconfiguration problem for the nonlinear equations of relative motion, it is more natural to use their periodic solutions.

Periodic solutions of the nonlinear relative dynamics with an eccentric reference orbit are used by Gurfil [24] for the initialization problem, in which given initial conditions of the nonlinear relative dynamics are adjusted by a single impulse to those of a periodic solution. The initialization problem with minimum velocity change is solved using an energy-matching condition. However, this method

Received 17 June 2009; revision received 29 December 2009; accepted for publication 30 December 2009.

*Mission Research Fellow, Research Institute for Sustainable Humanosphere, Gokasho, Uji; m-bando@rish.kyoto-u.ac.jp. Member AIAA.

†Professor, Department of Aeronautics and Astronautics, Graduate School of Engineering; ichikawa@kuaero.kyoto-u.ac.jp. Member AIAA.

is not applicable to a formation acquisition problem with a given relative orbit or to a reconfiguration problem. Periodic motion of the nonlinear relative dynamics is also studied by Sengupta et al. [25] using the gravity potential of the follower and its series expansion in Legendre polynomials. Periodic solutions of the nonlinear relative dynamics generated by two inertial elliptic orbits are used by Ketema [26] for a reconfiguration problem with two impulses. However, the relative orbits used in the formation problem are the first-order approximations of the original periodic orbits in three parameters concerning the difference of eccentricity vector, the offset for the center of a relative orbit, and the angle of inclination, and they coincide with elliptic relative orbits of the HCW equation.

The purpose of this paper is to formulate formation acquisition and reconfiguration problems for the nonlinear equations of relative motion along an eccentric orbit using their periodic solutions. First, the characterization results of [17] are extended to the case of an eccentric reference orbit. The relative motion of two satellites is periodic if the semimajor axes of their inertial orbits are equal. Using this fact, initial conditions of all periodic solutions of the nonlinear equations of relative motion are explicitly given in terms of the parameters of the follower's inertial orbit and two rotation angles between two perifocal reference systems. Setting the eccentricity of the leader satellite equal to zero, our results recover those of [17]. Our formation acquisition problem is to steer the follower from an arbitrary initial state to a given periodic relative orbit using a feedback controller. If the follower is initially in a periodic relative orbit, it becomes a reconfiguration problem. Feedback controllers are designed through a differential Riccati equation (DRE) of the TH system by taking penalty matrices as design parameters. The main performance index is the total velocity change or the L_1-norm of their control input, but the L_2-norm of the control input, the maximum of each component of the control input, and the settling time are also computed. For three examples, feedback controllers are designed, and controlled trajectories, control histories, and their total velocity changes are given. The performance indices of two examples are close to those of a reconfiguration problem of [15] concerning the TH system, which shows that the LQR controllers are equally effective for our new formation acquisition and reconfiguration problems.

To reduce the total velocity change of the control input generated by the LQR feedback controller, the NCVE property of the TH system is used [15–17]. The notion of NCVE was introduced by Priola and Zabczyk [27] for infinite-dimensional systems. A linear system is null-controllable with vanishing energy (also denoted by NCVE) if any state can be steered to the origin by a control with an arbitrarily small L_2-norm, as the control duration becomes arbitrarily large. The notion of NCVE was extended by Ichikawa [28] to discrete-time systems and periodic systems. The NCVE property of both HCW and TH systems was shown by Shibata and Ichikawa [15]. This property ensures the design of a feedback controller with an arbitrarily small L_2-norm through the LQR theory, taking a small (large) penalty matrix on state (control, respectively). It is shown in [15] that the total velocity change of the control input also decreases monotonically as the penalty on control increases. This property is also confirmed for our new formation acquisition and reconfiguration problems.

This paper is organized as follows. Section I is an introduction. Section II reviews the equations of relative motion and gives the characterization of initial conditions of all periodic solutions of the nonlinear relative dynamics. Section III gives formation acquisition and reconfiguration problems and discusses the design of feedback controllers. Section IV presents simulation results on three examples. Section V gives conclusions.

II. Equations of Relative Motion and Their Periodic Solutions

The equation of motion of a satellite subject to the gravitational force of the Earth and a control input is given by Newton's equation [4]:

$$\ddot{\boldsymbol{R}} = -\frac{\mu}{R^3}\boldsymbol{R} + \boldsymbol{u} \tag{1}$$

where $\boldsymbol{R}$ is the position vector of the satellite from the center of the Earth, μ is the gravitational parameter of the Earth, $R = |\boldsymbol{R}|$, and $\boldsymbol{u}$ is the control acceleration. If $\boldsymbol{u} = 0$ and the orbit of Eq. (1) is eccentric, then

$$R(t) = \frac{p}{1 + e\cos\theta(t)} \tag{2}$$

where $p = a(1 - e^2)$ is the semilatus rectum, a is the semimajor axis, e is the eccentricity of the orbit, and θ is the true anomaly. The period of the orbit is $T = 2\pi(a^3/\mu)^{1/2}$, and the orbital mean motion, which is the average of the orbit rate $\dot{\theta}$, is $n = (\mu/a^3)^{1/2}$. The following lemma for an eccentric orbit (R, θ) is useful for later developments.

Lemma 1.

$$p\dot{\theta}(t) = \left(\frac{\mu}{p}\right)^{1/2}(1 + e\cos\theta(t))^2$$

$$p\frac{\mathrm{d}}{\mathrm{d}t}\frac{\cos(\theta(t)+\beta)}{1 + e\cos\theta(t)} = -\left(\frac{\mu}{p}\right)^{1/2}[\sin(\theta(t)+\beta) + e\sin\beta]$$

$$p\frac{\mathrm{d}}{\mathrm{d}t}\frac{\sin(\theta(t)+\beta)}{1 + e\cos\theta(t)} = \left(\frac{\mu}{p}\right)^{1/2}[\cos(\theta(t)+\beta) + e\cos\beta]$$

where β is an arbitrary phase angle. The first equation follows from Kepler's second law concerning the area velocity [4], and the other two equalities are obtained by direct differentiation.

Now consider two satellites subject to the central gravity field of the Earth, one of which is flying in a given eccentric orbit denoted by (R_L, θ_L) and is referred to as a leader, and the other flying nearby is referred to as a follower. The relative motion of the follower with respect to the leader is given via Eq. (1) as follows:

$$\ddot{x} = 2\dot{\theta}_L\dot{y} + \ddot{\theta}_L y + \dot{\theta}_L^2 x + \frac{\mu}{R_L^2} - \frac{\mu}{R^3}(x + R_L) + u_x$$

$$\ddot{y} = -2\dot{\theta}_L\dot{x} - \ddot{\theta}_L x + \dot{\theta}_L^2 y - \frac{\mu}{R^3}y + u_y, \qquad \ddot{z} = -\frac{\mu}{R^3}z + u_z \tag{3}$$

where the coordinate system (x, y, z) is fixed at the center of mass of the leader; x, y, and z axes are along the radial direction, the flight direction of the leader, and the normal direction, respectively (see Fig. 1); $R = [(R_L + x)^2 + y^2 + z^2]^{1/2}$; and u_x, u_y, and u_z are the control accelerations.

Let a_L and $\boldsymbol{e}_L$ be the semimajor axis and the eccentricity vector, respectively, of the leader's orbit. Then the orbit is also denoted by $\Gamma_L = (a_L, \boldsymbol{e}_L)$. Assume that the follower is in an eccentric orbit $\Gamma = (a, \boldsymbol{e})$ in the inertial frame. Let (X, Y, Z) be its perifocal reference frame whose origin is the center of the earth, and the X axis is in the direction of the eccentricity vector $\boldsymbol{e}$. Assume first that two inertial orbits are coplanar, as shown in Fig. 1, in which $\boldsymbol{R}$ and $\boldsymbol{R}_L$ are the position vectors of the follower and the leader, respectively,

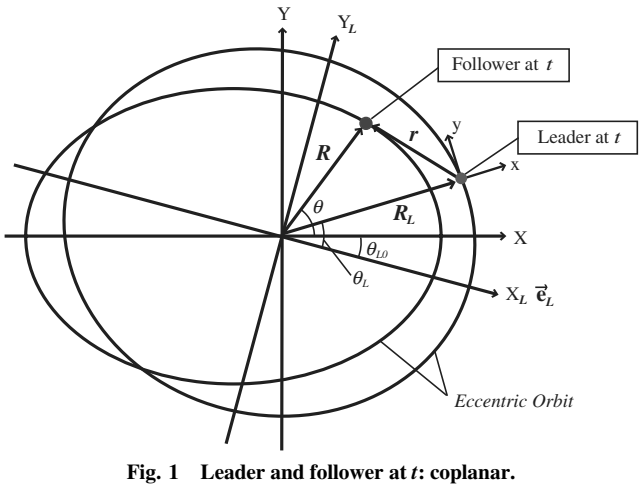

Fig. 1 Leader and follower at t: coplanar.

and $\boldsymbol{r}$ is the relative position vector. Let t_0 be the time at which the leader is in the direction of $\boldsymbol{e}$ (X axis). Let (R, θ) denote the eccentric orbit of the follower, and set $\theta_0 = \theta(t_0)$. Below, the initial conditions of Eq. (3) at t_0 will be calculated. Recall that the relative motion of the follower is periodic if and only if $a = a_L$, because in this case, the periods of the two eccentric orbits coincide.

Note that $\boldsymbol{r}(t)$ in the (X, Y, Z) coordinate system is given by

$$\boldsymbol{r}(t) = \boldsymbol{R}(t) - \boldsymbol{R}_L(t) = \begin{bmatrix} R(t)\cos\theta(t) - R_L(t)\cos(\theta_L(t) - \theta_{L0}) \\ R(t)\sin\theta(t) - R_L(t)\sin(\theta_L(t) - \theta_{L0}) \\ 0 \end{bmatrix} \tag{4}$$

where $\theta_{L0} = \theta_L(t_0)$ is the angle between $\boldsymbol{e}$ and $\boldsymbol{e}_L$. Note that the angular velocity of the rotating frame (x, y, z) is $\boldsymbol{\omega} = [0 \quad 0 \quad \dot{\theta}_L(t)]^T$. Hence, the derivatives of $\boldsymbol{r}(t)$ in the (X, Y, Z) and (x, y, z) frames denoted, respectively, by $\dot{\boldsymbol{r}}$ (or $\mathrm{d}\boldsymbol{r}/\mathrm{d}t$) and $\delta\boldsymbol{r}/\delta t$ are related by the following equation [4]:

$$\dot{\boldsymbol{r}} = \frac{\mathrm{d}\boldsymbol{r}}{\mathrm{d}t} = \frac{\delta\boldsymbol{r}}{\delta t} + \boldsymbol{\omega} \times \boldsymbol{r}$$

The relative velocity $\delta\boldsymbol{r}/\delta t$ expressed in the (X, Y, Z) coordinate system is given by

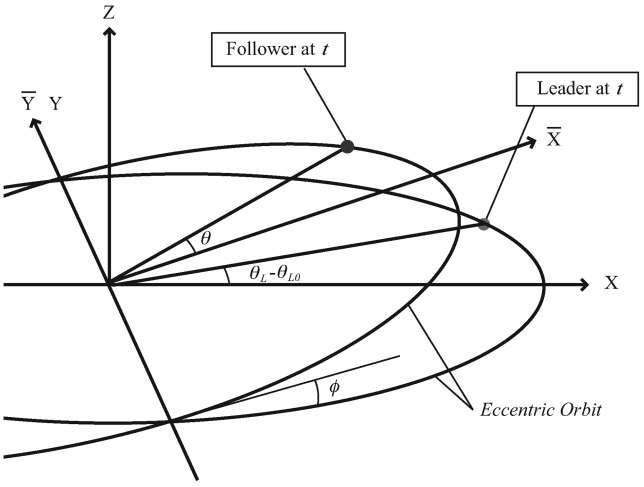

Fig. 3 Leader and follower at t: noncoplanar.

where the equality $(\mu/p)^{1/2} = na/(1-e^2)^{1/2}$ and Lemma 1 with $\beta = 0$ are used. Thus, the relative velocity at t_0 is

$$\frac{\delta\boldsymbol{r}}{\delta t}(t) = \dot{\boldsymbol{r}} - \boldsymbol{\omega} \times \boldsymbol{r}(t) = \dot{\boldsymbol{R}} - \dot{\boldsymbol{R}}_L - \boldsymbol{\omega} \times \boldsymbol{r}(t)$$

$$= \begin{bmatrix} -\frac{na}{(1-e^2)^{1/2}}\sin\theta(t) + \frac{n_L a_L}{(1-e_L^2)^{1/2}}[\sin(\theta_L(t) - \theta_{L0}) - e_L \sin\theta_{L0}] + \dot{\theta}_L(t)[R(t)\sin\theta(t) - R_L(t)\sin(\theta_L(t) - \theta_{L0})] \\ \frac{na}{(1-e^2)^{1/2}}(\cos\theta(t) + e) - \frac{n_L a_L}{(1-e_L^2)^{1/2}}[\cos(\theta_L(t) - \theta_{L0}) + e_L \cos\theta_{L0}] - \dot{\theta}_L(t)[R(t)\cos\theta(t) - R_L(t)\cos(\theta_L(t) - \theta_{L0})] \\ 0 \end{bmatrix} \tag{5}$$

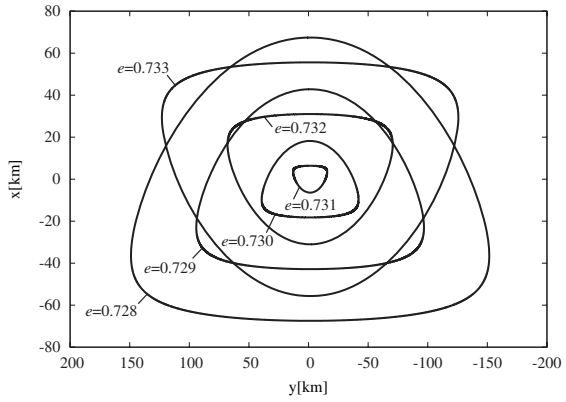

a) $\theta_{L0} = 0$, $\theta_0 = 0$

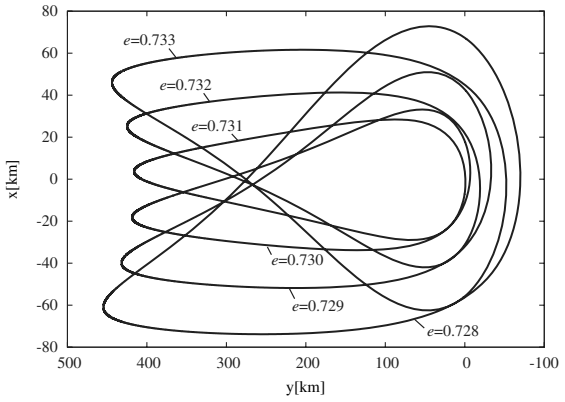

b) $\theta_{L0} = 0.1$, $\theta_0 = 0$

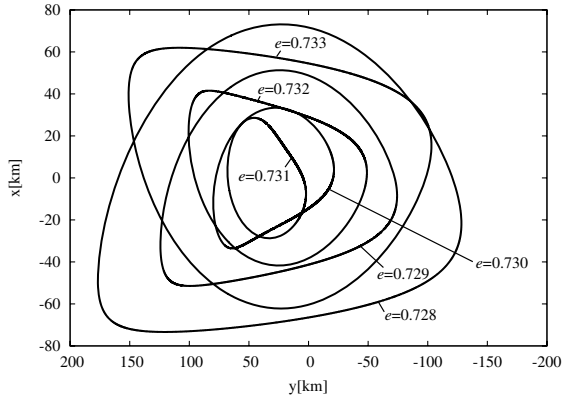

c) $\theta_{L0} = 0$, $\theta_0 = 0.1$

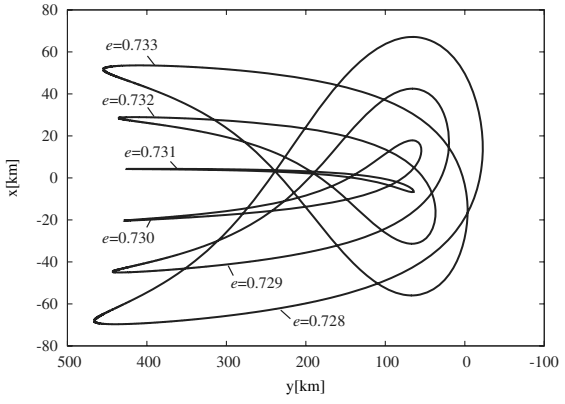

d) $\theta_{L0} = 0.1$, $\theta_0 = 0.1$

Fig. 2 Coplanar periodic relative orbits ($a_L = 24,616$ km, $e_L = 0.73074$).

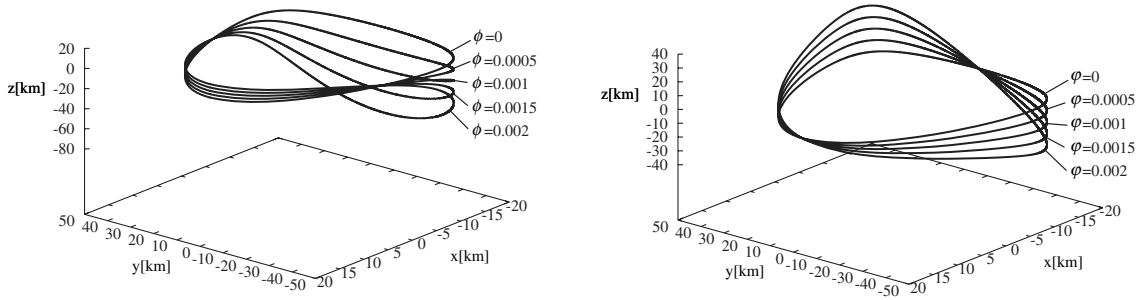

a) $e = 0.73$, $\theta_{L0} = 0$, $\theta_0 = 0$ **b)** $e = 0.73$, $\theta_{L0} = 0$, $\theta_0 = 0$

Fig. 4 Noncoplanar periodic relative orbits ($a_L = 24,616$ km, $e_L = 0.73074$).

$$\frac{\delta \boldsymbol{r}}{\delta t}(t_0) = \begin{bmatrix} -\frac{na}{(1-e^2)^{1/2}}\sin\theta_0 - \frac{n_L a_L}{(1-e_L^2)^{1/2}} e_L \sin\theta_{L0} + \frac{n_L}{(1-e_L^2)^{3/2}}(1+e_L\cos\theta_{L0})^2 \frac{a(1-e^2)}{1+e\cos\theta_0}\sin\theta_0 \\ \frac{na}{(1-e^2)^{1/2}}(\cos\theta_0 + e) - \frac{n_L}{(1-e_L^2)^{3/2}}(1+e_L\cos\theta_{L0})^2 \frac{a(1-e^2)}{1+e\cos\theta_0}\cos\theta_0 \\ 0 \end{bmatrix} \tag{6}$$

Because $\delta \boldsymbol{r}/\delta t$ in two coordinate systems (X, Y, Z) and (x, y, z) coincide at t_0, Eq. (6) is also the relative velocity in the (x, y, z) coordinate system. Hence, Eq. (4) with $t = t_0$ and Eq. (6) give the initial positions and velocities at t_0: that is,

$$\begin{bmatrix} x(t_0) \\ y(t_0) \\ z(t_0) \end{bmatrix} = \begin{bmatrix} \frac{A(1-e^2)}{1+e\cos\theta_0}\cos\theta_0 - \frac{a_L(1-e_L^2)}{1+e_L\cos\theta_{L0}} \\ \frac{a(1-e^2)}{1+e\cos\theta_0}\sin\theta_0 \\ 0 \end{bmatrix} \tag{7}$$

$$\begin{bmatrix} \dot{x}(t_0) \\ \dot{y}(t_0) \\ \dot{z}(t_0) \end{bmatrix} = \begin{bmatrix} -\frac{na}{(1-e^2)^{1/2}}\sin\theta_0 - \frac{n_L a_L}{(1-e_L^2)^{1/2}} e_L \sin\theta_{L0} + \frac{n_L}{(1-e_L^2)^{3/2}}(1+e_L\cos\theta_{L0})^2 \frac{a(1-e^2)}{1+e\cos\theta_0}\sin\theta_0 \\ \frac{na}{(1-e^2)^{1/2}}(\cos\theta_0 + e) - \frac{n_L}{(1-e_L^2)^{3/2}}(1+e_L\cos\theta_{L0})^2 \frac{a(1-e^2)}{1+e\cos\theta_0}\cos\theta_0 \\ 0 \end{bmatrix} \tag{8}$$

Equations (7) and (8) are general initial conditions corresponding to an arbitrary eccentric orbit of the follower, and the substitution of $a = a_L$ and $n = n_L$ yields a periodic solution of Eq. (3).

Theorem 1. Let $\Gamma = (a_L, \boldsymbol{e})$ be an inertial coplanar eccentric orbit of the follower. Let t_0 be the time at which the leader is in the direction of $\boldsymbol{e}$, and let $\theta_0 = \theta(t_0)$. Then the relative motion of the follower with respect to the leader is periodic, and the initial conditions of Eq. (3) at t_0 are given by

$$\begin{bmatrix} x(t_0) \\ y(t_0) \\ z(t_0) \end{bmatrix} = \begin{bmatrix} \frac{a_L(1-e^2)}{1+e\cos\theta_0}\cos\theta_0 - \frac{a_L(1-e_L^2)}{1+e_L\cos\theta_{L0}} \\ \frac{a_L(1-e^2)}{1+e\cos\theta_0}\sin\theta_0 \\ 0 \end{bmatrix} \tag{9}$$

$$\begin{bmatrix} \dot{x}(t_0) \\ \dot{y}(t_0) \\ \dot{z}(t_0) \end{bmatrix} = \begin{bmatrix} -\frac{n_L a_L}{(1-e^2)^{1/2}}\sin\theta_0 - \frac{n_L a_L}{(1-e_L^2)^{1/2}} e_L \sin\theta_{L0} + \frac{n_L}{(1-e_L^2)^{3/2}}(1+e_L\cos\theta_{L0})^2 \frac{a_L(1-e^2)}{1+e\cos\theta_0}\sin\theta_0 \\ \frac{n_L a_L}{(1-e^2)^{1/2}}(\cos\theta_0 + e) - \frac{n_L}{(1-e_L^2)^{3/2}}(1+e_L\cos\theta_{L0})^2 \frac{a_L(1-e^2)}{1+e\cos\theta_0}\cos\theta_0 \\ 0 \end{bmatrix} \tag{10}$$

Initial conditions in this theorem with $e_L = 0$ recover those in [17]. Using Eqs. (9) and (10), periodic solutions of Eq. (3) corresponding to $a_L = 24,616$ km and $e_L = 0.73074$ with parameter e are depicted in Figs. 2a–2d. In Fig. 2a, the leader and the follower are on the X axis at $t = 0$. If $e < e_L$, the perigee height is larger for the follower orbit and $x(0) > 0$. If $e > e_L$, then $x(0) < 0$ and the periodic orbit is inverted.

Now consider noncoplanar orbits of the follower and their associated initial conditions of Eq. (3). General noncoplanar orbits of the follower can be generated by two successive rotations $C_2(\phi)$ and $C_1(\psi)$ (see Fig. 3), where

$$C_1(\psi) = \begin{bmatrix} 1 & 0 & 0 \\ 0 & \cos\psi & \sin\psi \\ 0 & -\sin\psi & \cos\psi \end{bmatrix}$$

$$C_2(\phi) = \begin{bmatrix} \cos\phi & 0 & -\sin\phi \\ 0 & 1 & 0 \\ \sin\phi & 0 & \cos\phi \end{bmatrix}$$

In fact, let $(\bar{X}, \bar{Y}, \bar{Z})$ and $(\tilde{X}, \tilde{Y}, \tilde{Z})$ be the perifocal reference frames obtained by rotating (X, Y, Z) around the Y axis by $-\phi$ and then around the $\bar{X}$ axis by $-\psi$ successively: i.e., $C_2(\phi)$: $(\bar{X}, \bar{Y}, \bar{Z}) \to (X, Y, Z)$ and $C_1(\psi)$: $(\tilde{X}, \tilde{Y}, \tilde{Z}) \to (\bar{X}, \bar{Y}, \bar{Z})$. The position vector of the follower at time t in the $(\tilde{X}, \tilde{Y}, \tilde{Z})$ coordinate system is given by

$$\boldsymbol{R}(t) = \begin{bmatrix} R(t)\cos\theta(t) \\ R(t)\sin\theta(t) \\ 0 \end{bmatrix}$$

and in the (X, Y, Z) coordinate system is given by

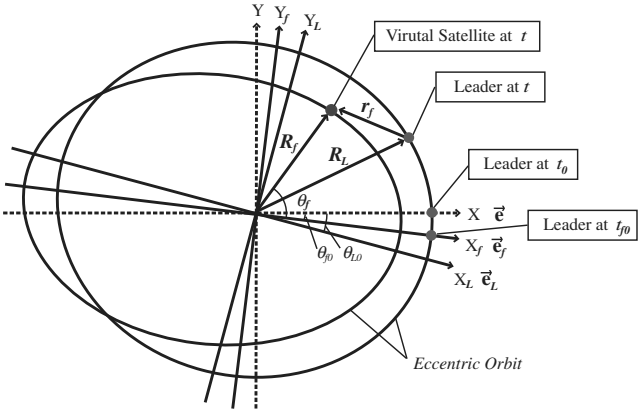

Fig. 5 Leader and virtual satellite at t: coplanar.

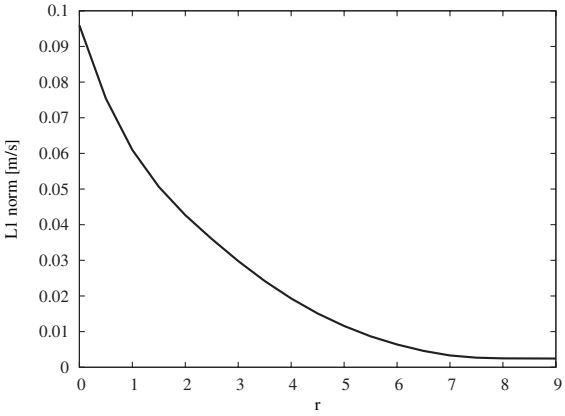

Fig. 6 L_1-norm.

$$\boldsymbol{R}(t) = C_2(\phi)C_1(\psi)\begin{bmatrix} R(t)\cos\theta(t) \\ R(t)\sin\theta(t) \\ 0 \end{bmatrix} = \begin{bmatrix} R(t)\cos\theta(t)\cos\phi + R(t)\sin\theta(t)\sin\phi\sin\psi \\ R(t)\sin\theta(t)\cos\psi \\ R(t)\cos\theta(t)\sin\phi - R(t)\sin\theta(t)\cos\phi\sin\psi \end{bmatrix}$$

Hence, the relative position vector $\boldsymbol{r}$ in the (X, Y, Z) coordinate system becomes

$$\boldsymbol{r}(t) = \begin{bmatrix} R(t)\cos\theta(t)\cos\phi + R(t)\sin\theta(t)\sin\phi\sin\psi - R_L(t)\cos(\theta_L(t) - \theta_{L0}) \\ R(t)\sin\theta(t)\cos\psi - R_L(t)\sin(\theta_L(t) - \theta_{L0}) \\ R(t)\cos\theta(t)\sin\phi - R(t)\sin\theta(t)\cos\phi\sin\psi \end{bmatrix} \tag{11}$$

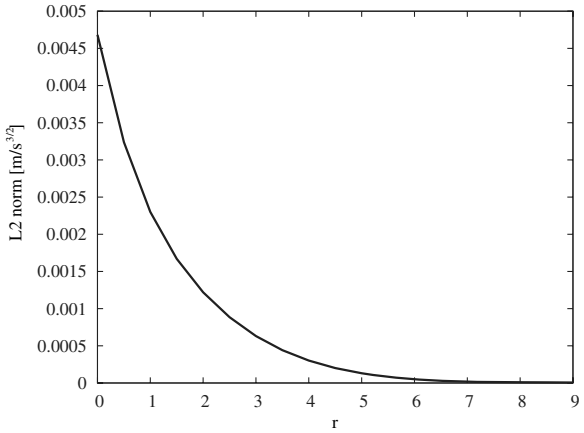

Fig. 7 L_2-norm.

The relative velocity expressed in the (X, Y, Z) coordinate system is then

$$\frac{\delta \boldsymbol{r}(t)}{\delta t} = \dot{\boldsymbol{r}} - \boldsymbol{\omega} \times \boldsymbol{r}(t) = \begin{bmatrix} -\frac{na}{(1-e^2)^{1/2}}\sin\theta(t)\cos\phi + \frac{na}{(1-e^2)^{1/2}}(\cos\theta(t) + e)\sin\phi\sin\psi + \frac{n_L a_L}{(1-e_L^2)^{1/2}}[\sin(\theta_L(t) - \theta_{L0}) - e_L\sin\theta_{L0}] \\ \frac{na}{(1-e^2)^{1/2}}(\cos\theta(t) + e)\cos\psi - \frac{n_L a_L}{(1-e_L^2)^{1/2}}[\cos(\theta_L(t) - \theta_{L0}) + e_L\cos\theta_{L0}] \\ -\frac{na}{(1-e^2)^{1/2}}\sin\theta(t)\sin\phi - \frac{na}{(1-e^2)^{1/2}}(\cos\theta(t) + e)\cos\phi\sin\psi \end{bmatrix}$$
$$+ \begin{bmatrix} \dot{\theta}_L(t)[R(t)\sin\theta(t)\cos\psi - R_L(t)\sin(\theta_L(t) - \theta_{L0})] \\ -\dot{\theta}_L(t)[R(t)\cos\theta(t)\cos\phi + R(t)\sin\theta(t)\sin\phi\sin\psi - R_L(t)\cos(\theta_L(t) - \theta_{L0})] \\ 0 \end{bmatrix} \tag{12}$$

Hence, the initial conditions at t_0 are given by

Table 1 Parameters of eccentric orbit

Constants	Values
R_e	6378 km
μ	398, 601 km^3/s^2
h_p	250 km
h_a	36226 km
e	0.73074
a_L	24616 km
T	38436 s

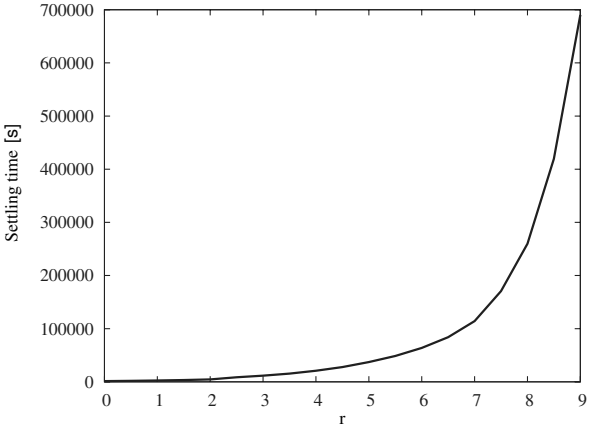

Fig. 8 Settling time.

$$\begin{bmatrix} x(t_0) \\ y(t_0) \\ z(t_0) \end{bmatrix} = \begin{bmatrix} \frac{a(1-e^2)}{1+e\cos\theta_0}\cos\theta_0\cos\phi + \frac{a(1-e^2)}{1+e\cos\theta_0}\sin\theta_0\sin\phi\sin\psi - \frac{a_L(1-e_L^2)}{1+e_L\cos\theta_{L0}} \\ \frac{a(1-e^2)}{1+e\cos\theta_0}\sin\theta_0\cos\psi \\ \frac{a(1-e^2)}{1+e\cos\theta_0}\cos\theta_0\sin\phi - \frac{a(1-e^2)}{1+e\cos\theta_0}\sin\theta_0\cos\phi\sin\psi \end{bmatrix} \tag{13}$$

$$\begin{bmatrix} \dot{x}(t_0) \\ \dot{y}(t_0) \\ \dot{z}(t_0) \end{bmatrix} = \begin{bmatrix} -\frac{na}{(1-e^2)^{1/2}}\sin\theta_0\cos\phi + \frac{na}{(1-e^2)^{1/2}}(\cos\theta_0 + e)\sin\phi\sin\psi - \frac{n_L a_L}{(1-e_L^2)^{1/2}}e_L\sin\theta_{L0} \\ \frac{na}{(1-e^2)^{1/2}}(\cos\theta_0 + e) \\ -\frac{na}{(1-e^2)^{1/2}}\sin\theta_0\sin\phi \end{bmatrix} + \begin{bmatrix} \frac{n_L}{(1-e_L^2)^{3/2}}(1+e_L\cos\theta_{L0})^2\frac{a(1-e^2)}{1+e\cos\theta_0}\sin\theta_0\cos\phi \\ -\frac{n_L}{(1-e_L^2)^{3/2}}(1+e_L\cos\theta_{L0})^2\frac{a(1-e^2)}{1+e\cos\theta_0}(\cos\theta_0\cos\phi + \sin\theta_0\sin\phi\sin\psi) \\ 0 \end{bmatrix} \tag{14}$$

Note that Eqs. (13) and (14) are reduced to Eqs. (7) and (8) if $\phi = 0$ and $\psi = 0$. Setting $a = a_L$ and $n = n_L$, initial conditions of a periodic solution of Eq. (3) are obtained.

Theorem 2. Let $\Gamma = (a_L, \boldsymbol{e}, \phi, \psi)$ be a noncoplanar eccentric orbit of the follower. Let t_0 be the time at which the leader is in the direction of $P\boldsymbol{e}$, and let $\theta_0 = \theta(t_0)$, where P is the rotation defined by $C_2(\phi)C_1(\psi)$ onto the orbit plane of the leader. Then the relative motion of the follower with respect to the leader is periodic, and the initial conditions of Eq. (3) at t_0 are given by

$$\begin{bmatrix} x(t_0) \\ y(t_0) \\ z(t_0) \end{bmatrix} = \begin{bmatrix} \frac{a_L(1-e^2)}{1+e\cos\theta_0}\cos\theta_0\cos\phi + \frac{a_L(1-e^2)}{1+e\cos\theta_0}\sin\theta_0\sin\phi\sin\psi - \frac{a_L(1-e_L^2)}{1+e_L\cos\theta_{L0}} \\ \frac{a_L(1-e^2)}{1+e\cos\theta_0}\sin\theta_0\cos\psi \\ \frac{a_L(1-e^2)}{1+e\cos\theta_0}\cos\theta_0\sin\phi - \frac{a_L(1-e^2)}{1+e\cos\theta_0}\sin\theta_0\cos\phi\sin\psi \end{bmatrix} \tag{15}$$

and

$$\begin{bmatrix} \dot{x}(t_0) \\ \dot{y}(t_0) \\ \dot{z}(t_0) \end{bmatrix} = \begin{bmatrix} -\frac{n_L a_L}{(1-e^2)^{1/2}}\sin\theta_0\cos\phi + \frac{n_L a_L}{(1-e^2)^{1/2}}(\cos\theta_0 + e)\sin\phi\sin\psi - \frac{n_L a_L}{(1-e_L^2)^{1/2}}e_L\sin\theta_{L0} \\ \frac{n_L a_L}{(1-e^2)^{1/2}}(\cos\theta_0 + e) \\ -\frac{n_L a_L}{(1-e^2)^{1/2}}\sin\theta_0\sin\phi \end{bmatrix} + \begin{bmatrix} \frac{n_L a_L}{(1-e_L^2)^{3/2}}(1+e_L\cos\theta_{L0})^2\frac{(1-e^2)}{1+e\cos\theta_0}\sin\theta_0\cos\phi \\ -\frac{n_L a_L}{(1-e_L^2)^{3/2}}(1+e_L\cos\theta_{L0})^2\frac{(1-e^2)}{1+e\cos\theta_0}(\cos\theta_0\cos\phi + \sin\theta_0\sin\phi\sin\psi) \\ 0 \end{bmatrix} \tag{16}$$

Initial conditions in the theorem with $e_L = 0$ recover those of [17]. Periodic relative orbits generated by the rotation of a coplanar orbit around the Y and X axes, respectively, are given in Figs. 4a and 4b.

The perifocal reference frame of an orbit is determined from the geocentric-equatorial reference frame using the rotation matrix $C_3(\omega)C_1(i)C_3(\Omega)$, where Ω is the right ascension of the ascending node, i is the inclination of the orbit plane, and ω is the argument of the perigee. The rotation angles ϕ and ψ are then determined from the relative Euler angles of the two perifocal reference frames of the leader and follower orbits.

The linearized equations of Eq. (3) at the null solution $x = y = z = 0$ are given by

$$\ddot{x} = 2\dot{\theta}_L\dot{y} + \ddot{\theta}_L y + \left(\dot{\theta}_L^2 + \frac{2\mu}{R_L^3}\right)x + u_x$$
$$\ddot{y} = -2\dot{\theta}_L\dot{x} - \ddot{\theta}_L x + \left(\dot{\theta}_L^2 - \frac{\mu}{R_L^3}\right)y + u_y, \qquad \ddot{z} = -\frac{\mu}{R_L^3}z + u_z \tag{17}$$

which are known as Tschauner–Hempel equations [20]. Defining

$$\boldsymbol{x} = [\,x \quad y \quad \dot{x} \quad \dot{y} \quad z \quad \dot{z}\,]^T, \qquad \boldsymbol{u} = [\,u_x \quad u_y \quad u_z\,]^T$$

the TH equations in the state-space form become

$$\dot{\boldsymbol{x}} = A(t)\boldsymbol{x} + B\boldsymbol{u} \tag{18}$$

where

$$A(t) = \begin{bmatrix} 0 & 0 & 1 & 0 & 0 & 0 \\ 0 & 0 & 0 & 1 & 0 & 0 \\ \dot{\theta}_L^2 + 2\mu/R_L^3 & 0 & \ddot{\theta}_L & 2\dot{\theta}_L & 0 & 0 \\ -\ddot{\theta}_L & \dot{\theta}_L^2 - \mu/R_L^3 & -2\dot{\theta}_L & 0 & 0 & 0 \\ 0 & 0 & 0 & 0 & 0 & 1 \\ 0 & 0 & 0 & 0 & -\mu/R_L^3 & 0 \end{bmatrix}$$

$$B = \begin{bmatrix} 0 & 0 & 0 \\ 0 & 0 & 0 \\ 1 & 0 & 0 \\ 0 & 1 & 0 \\ 0 & 0 & 0 \\ 0 & 0 & 1 \end{bmatrix}$$

Equation (3) is rewritten in a semilinear form as

$$\dot{\boldsymbol{x}} = A(t)\boldsymbol{x} + B\boldsymbol{u} + Bg(\boldsymbol{x}) \tag{19}$$

where

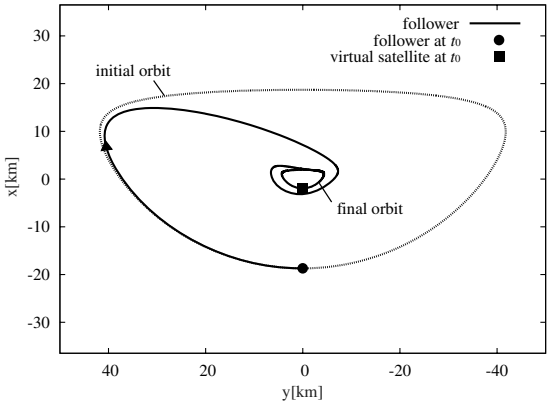

Fig. 9 Controlled trajectory: coplanar.

$$\dot{\boldsymbol{x}}_f = A(t)\boldsymbol{x}_f + Bg(\boldsymbol{x}_f), \qquad \boldsymbol{x}_f(t_{f0}) = \boldsymbol{x}_{f0} \tag{21}$$

where $\boldsymbol{x}_{f0}$ is determined by γ_f. Without loss of generality, the inequality $t_0 > t_{f0}$ is assumed. For simplicity, consider a coplanar orbit $\gamma_f = (a_L, \boldsymbol{e}_f, t_{f0}, \theta_{f0})$ (see Fig. 5). Then the relative positions of the virtual satellite at t in the perifocal reference frame of the initial orbit $\Gamma = (a, \boldsymbol{e})$ are given by

$$\begin{aligned}\boldsymbol{r}(t) &= \boldsymbol{R}_f(t) - \boldsymbol{R}_L(t) \\ &= \begin{bmatrix} R_f(t)\cos(\theta_f(t) - \theta_{0f}) - R_L(t)\cos(\theta_L(t) - \theta_{L0}) \\ R_f(t)\sin(\theta_f(t) - \theta_{0f}) - R_L(t)\sin(\theta_L(t) - \theta_{L0}) \\ 0 \end{bmatrix}\end{aligned}$$

where θ_{0f} is the angle between $\boldsymbol{e}$ and $\boldsymbol{e}_f$, and

$$g(\boldsymbol{x}) = [\,\mu/R_L^2 - \mu(x + R_L)/R^3 - 2\mu x/R_L^3 \quad -\mu y(1/R^3 - 1/R_L^3) \quad -\mu z(1/R^3 - 1/R_L^3)\,]^T$$

The TH system (18) will be used to design feedback controllers.

III. Formation Acquisition and Reconfiguration Problems

In this section, formation and reconfiguration problems based on the periodic relative orbits are considered. First, a characterization of relative orbits is given. Let (X_0, Y_0, Z_0) be an inertial reference frame such that the (X_0, Y_0) plane coincides with the orbit plane of the leader. Let $\Gamma_L = (a_L, \boldsymbol{e}_L)$ be the inertial orbit of the leader, and let $\Gamma = (a_0, \boldsymbol{e})$ be a coplanar inertial orbit of the follower. Then the relative orbit is determined by the initial time t_0 and the initial true anomaly θ_0, and hence it will be denoted by $\gamma = (a_0, \boldsymbol{e}, t_0, \theta_0)$. Similarly, the relative orbit corresponding to a noncoplanar inertial orbit is denoted by $\gamma = (a_0, \boldsymbol{e}, t_0, \theta_0, \phi, \psi)$ if the angles of successive rotations of the coplanar orbit around the Y axis and the $\bar{X}$ axis are $-\phi$ and $-\psi$, respectively. Our formation acquisition problem is described as follows. For a given initial relative orbit $\gamma_0 = (a, \boldsymbol{e}, t_0, \theta_0, \phi_0, \psi_0)$ and a final periodic orbit $\gamma_f = (a_L, \boldsymbol{e}_f, t_{f0}, \theta_{f0}, \phi_f, \psi_f)$, find a feedback control such that the solution of Eq. (19) starting from the initial orbit tracks γ_f asymptotically. The performance index of the controller is the total velocity change represented by the L_1-norm of its control input. If, in particular, the initial orbit is periodic, i.e., $\gamma_0 = (a_L, \boldsymbol{e}_0, t_0, \theta_0, \phi_0, \psi_0)$, it is a reconfiguration problem.

Note that two orbits γ_0 and γ_f in general have different initial times, which is inconvenient for control purposes. Below, it will be shown how to calculate the relative state of the final orbit at t_0. Recall that the relative dynamics of the follower are given by Eq. (19) so that

$$\dot{\boldsymbol{x}} = A(t)\boldsymbol{x} + B\boldsymbol{u} + Bg(\boldsymbol{x}), \qquad \boldsymbol{x}(t_0) = \boldsymbol{x}_0 \tag{20}$$

where the initial condition $\boldsymbol{x}_0$ is determined by γ_0. To track γ_f, a virtual satellite is introduced, which follows the free motion of Eq. (19): i.e.,

Table 2 Performance indices: example 1

Performance indices	Values
$\|u\|_1$	3.3184 m/s
$\|u\|_2$	1.7635×10^{-2} m/s$^{3/2}$
T_s	114,301 s
$u_x^{\max}$	2.1655×10^{-4} m/s^2
$u_y^{\max}$	1.7352×10^{-4} m/s^2
$\|g(\boldsymbol{x}) - g(\boldsymbol{x}_f)\|_1$	1.3452×10^{-2} m/s
$\|u_n\|_1$	3.3198 m/s

$$R_f(t) = \frac{A_L(1 - e_f^2)}{(1 + e_f \cos\theta_f(t))}$$

Note that θ_{0f} is not equal to $\theta_f(t_0)$ or to $\theta_f(t_{f0})$. As in the previous section,

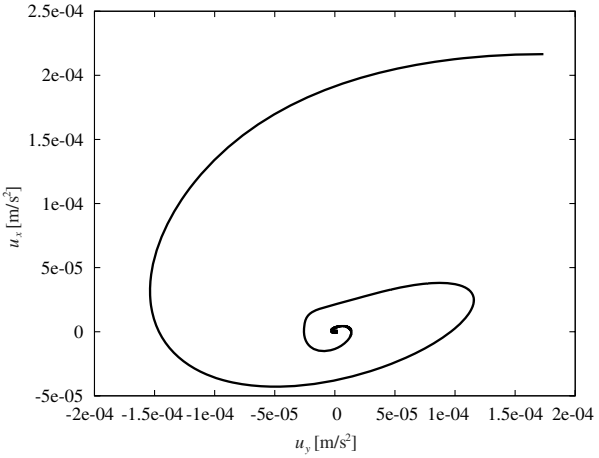

Fig. 10 Locus of control vector: coplanar.

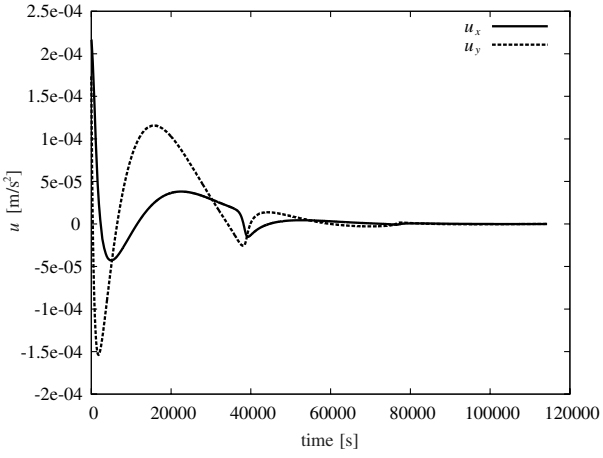

Fig. 11 History of control input: coplanar.

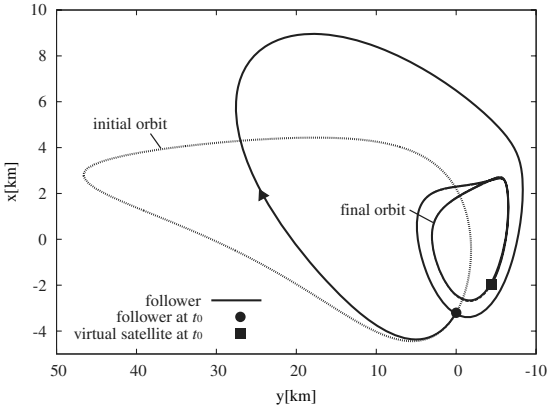

Fig. 12 Controlled trajectory: coplanar/general.

$$\boldsymbol{r}_f(t_0) = \begin{bmatrix} R_f(t_0)\cos(\theta_f(t_0) - \theta_{0f}) - \frac{a_L(t_0)(1-e_L^2)}{1+e_L\cos\theta_{L0}} \\ R_f(t_0)\sin(\theta_f(t_0) - \theta_{0f}) \\ 0 \end{bmatrix} \tag{22}$$

and

$$\frac{\delta \boldsymbol{r}_f(t_0)}{\delta t} = \dot{\boldsymbol{r}}_f(t_0) - \boldsymbol{\omega} \times \boldsymbol{r}_f(t_0)$$
$$= \begin{bmatrix} -\frac{n_L a_L}{(1-e_f^2)^{1/2}}[\sin(\theta_f(t_0) - \theta_{0f}) - e_f \sin\theta_{0f}] - \frac{n_L a_L}{(1-e_L^2)^{1/2}} e_L \sin\theta_{L0} + \frac{n_L}{(1-e_L^2)^{3/2}}(1 + e_L\cos\theta_{L0})^2 R_f(t_0)\sin(\theta_f(t_0) - \theta_{0f}) \\ \frac{n_L a_L}{(1-e_f^2)^{1/2}}[\cos(\theta_f(t_0) - \theta_{0f}) + e_f\cos\theta_{0f}] - \frac{n_L}{(1-e_L^2)^{3/2}}(1 + e_L\cos\theta_{L0})^2 R_f(t_0)\cos(\theta_f(t_0) - \theta_{0f}) \\ 0 \end{bmatrix} \tag{23}$$

where Lemma 1 with $\beta = -\theta_{0f}$ is used. The true anomaly $\theta_f(t_0)$ is determined by Kepler's time equation,

$$n(t_0 - t_p) = E_f(t_0) - e_f \sin E_f(t_0)$$

and the following relation:

$$\cos\theta_f(t_0) = \frac{\cos E_f(t_0) - e_f}{1 - e_f \cos E_f(t_0)}$$

where E_f is the eccentric anomaly, and the perigee passage time t_p is given by

$$n(t_{f0} - t_p) = E_f(t_{f0}) - e_f \sin E_f(t_{f0})$$
$$\cos\theta_f(t_{f0}) = \frac{\cos E_f(t_{f0}) - e_f}{1 - e_f \cos E_f(t_{f0})}$$

The initial condition $\boldsymbol{x}_f(t_0)$ is then obtained by rearranging Eqs. (22) and (23). When γ_f is noncoplanar, the relative position and velocity at t_0 can be derived using rotation matrices.

Now feedback controllers such that $\boldsymbol{x}(t) - \boldsymbol{x}_f(t) \to 0$ as $t \to \infty$ are designed. Introduce the error dynamics

$$\dot{\boldsymbol{\epsilon}} = A(t)\boldsymbol{\epsilon} + B\boldsymbol{u} + B[g(\boldsymbol{x}) - g(\boldsymbol{x}_f)] \tag{24}$$

where $\boldsymbol{\epsilon} = \boldsymbol{x} - \boldsymbol{x}_f$. As a main performance index, the total velocity change (L_1-norm) of a controller, which represents the fuel consumption, is employed. Recall that $(A(t), B)$ is null-controllable with vanishing energy [15]. This is a property by which any state can be steered to the origin with an arbitrary small amount of control energy in the L_2 (square integral) sense, provided that the time duration is free. Consider the DRE

$$-\dot{X} = A^T X(t) + XA(t) + Q - XBR^{-1}B^T X \tag{25}$$

and the feedback controller

$$\boldsymbol{u} = -R^{-1}B^T X(t)\boldsymbol{\epsilon} \tag{26}$$

where Q is nonnegative and R is positive. If $\sqrt{Q}$ and A are detectable, the DRE has a unique T-periodic stabilizing solution [29]. Its initial condition $X(0)$ is calculated recursively by

$$-\dot{X}_k = A^T X_k(t) + X_k A(t) + Q - X_k B R^{-1} B^T X_k$$
$$X_k(T) = X_{k-1}(0)$$

where $X_0(T) = 0$. In fact, $X_k(0)$ converges monotonically to $X(0)$.

In [15], the feedback controller (26) is applied to the reconfiguration problem for the TH error system. Because of the NCVE property, its L_2-norm converges to zero as Q goes to zero (or, equivalently, as R increases to infinity). In the next section, the feedback controller (26) is employed for the reconfiguration problem of the nonlinear system (20), and the total velocity change will be computed. Instead of the feedback controller (26), the nonlinear feedback controller

$$\boldsymbol{u}_n = -R^{-1}B^T X\boldsymbol{\epsilon} - [g(\boldsymbol{x}) - g(\boldsymbol{x}_f)] \tag{27}$$

[which stabilizes Eq. (24) globally] can be employed. When the relative orbit is small, the total velocity changes of feedback controllers (26) and (27) are almost identical, as shown in the next section.

IV. Simulation Results

To see the effects of large eccentricity on relative orbits, an elliptic orbit of the leader with eccentricity $e = 0.73074$ considered in [15] is chosen. Table 1 shows the parameters of this orbit, where h_p and h_a are the height of the perigee and apogee, respectively. The semimajor axis is $a_L = 24,616$ km and the period of this orbit is $T = 38436$ s. The radius of the Earth R_e and the gravitational constant of the Earth μ are also given in the table. Let $(\boldsymbol{i}, \boldsymbol{j}, \boldsymbol{k})$ be the basis vectors of the inertial frame (X_0, Y_0, Z_0).

Example 1. Coplanar Formation: A Synchronized Case. Let $\gamma_0 = (a_L, 0.7315\boldsymbol{i}, 0, 0)$ and $\gamma_f = (a_L, 0.73082\boldsymbol{i}, 0, 0)$ be two periodic relative orbits, and consider the reconfiguration from γ_0 to γ_f. In this case, (X_0, Y_0, Z_0) is the perifocal reference frame of the two orbits, and the leader, follower, and virtual satellite are initially on the X_0 axis so that $t_0 = t_{f0} = 0$. Using Eqs. (9) and (10), the initial conditions of the nonlinear system (20) and (21) are given, respectively, by

$$\boldsymbol{x}_0 = [-18.707 \;\; 0.00000 \;\; 0.00000 \;\; 0.04546 \;\; 0.00000 \;\; 0.00000]$$
$$\boldsymbol{x}_{f0} = [-1.9692 \;\; 0.00000 \;\; 0.00000 \;\; 0.0047829 \;\; 0.00000 \;\; 0.00000]$$

This example does not involve the out-of-plane motion, and hence the four-dimensional subsystems of Eq. (19) are used for simulations. As in [15], Q and R in Eq. (25) are assumed to be diagonal, i.e., $Q = \mathrm{diag}(q_i)$ and $R = 10^r I$ with $q_i = 1.0 \times 10^{-9}$ $(i = 1, 2)$, and $q_i = 0$ $i = 3, 4)$. The L_1 and L_2-norms of the control input and the settling time are given as functions of the parameter r and are depicted in Figs. 6–8. Here, the settling time is defined as the first time after which inequalities $|x - x_f|$, $|y - y_f| < 10^{-6} r_{\min}$, $|\dot{x} - \dot{x}_f|$, and $|\dot{y} - \dot{y}_f| < 10^{-6} v_{\min}$ are satisfied, where $r_{\min}$ is the minimum distance of a point in the final orbit from its center, and $v_{\min}$

is the minimum velocity of the follower in the final orbit. The parameter $r = 7$ is selected to make the settling time less than three orbits ($3T$). The controller (26) is applied to the nonlinear system (20). Figure 9 shows two orbits, γ_0 and γ_f, and the controlled trajectory. Performance indices are given in Table 2. The total velocity change for the reconfiguration is shown as the L_1-norm and is 3.3184 m/s, and the settling time $T_s = 114,301$ s. The control accelerations are in the ranges of

$$-4.2863 \times 10^{-5} < u_x < 2.1655 \times 10^{-4} \text{ m/s}^2$$

and

$$-1.5378 \times 10^{-4} < u_y < 1.7352 \times 10^{-4} \text{ m/s}^2$$

The locus of the vector $\boldsymbol{u}_{\text{in}} = [\, u_x \quad u_y \,]^T$ and the histories of the inputs u_x and u_y are given, respectively, in Figs. 10 and 11. These figures indicate a specification for the thruster of the in-plane motion. The L_1-norm of the nonlinear term $g(\boldsymbol{x}) - g(\boldsymbol{x}_f)$ is 1.3452×10^{-2} m/s and is less than 1% of the total velocity change. The nonlinear feedback (27) is also applied to the system (20). The controlled trajectory is almost identical with that in Fig. 9, and its L_1-norm is 3.3198 m/s. The initial value of the stabilizing T-periodic solution of the DRE is given by

$$X(0) = \begin{bmatrix} 0.040315 & -0.0021630 & 3.1708 & 16.458 \\ -0.0021629 & 0.00028889 & -0.41876 & -0.85139 \\ 3.1708 & -0.41876 & 612.10 & 1251.3 \\ 16.458 & -0.85139 & 1251.3 & 6728.6 \end{bmatrix}$$

Example 2. Coplanar Formation: A General Case. Consider the initial and final orbits given by $\gamma_0 = (a_L, 0.73087\boldsymbol{i}', 0, 0)$ and $\gamma_f = (a_L, 0.73082\boldsymbol{i}, -0.71462, 0)$, where $\boldsymbol{i}'$ is the 10^{-3} radian rotation of $\boldsymbol{i}$ in the positive direction. Thus, the X_0 axis is the perigee direction of the leader and virtual satellites. The initial conditions of the follower and the virtual satellite at $t_0 = 0$ and $t_{f0} = -0.730870$, respectively, are given by

$$\boldsymbol{x}_0(0) = [-3.2017 \;\; 0.00000 \;\; 0.0047382 \;\; 0.0077778 \;\; 0.00000 \;\; 0.00000]$$

$$\boldsymbol{x}_{f0}(-0.73087) = [-1.9692 \;\; 0.00000 \;\; 0.00000 \;\; 0.0047829 \;\; 0.00000 \;\; 0.00000]$$

In view of Eqs. (9) and (10), the state of the virtual satellite at $t_0 = 0$ is given by

$$\boldsymbol{x}_f(0) = [-1.9721 \;\; -4.4137 \;\; -0.0028657 \;\; 0.0047860 \;\; 0.00000 \;\; 0.00000]$$

In this example, the penalty parameters of Example 1 are used. Figure 12 gives two orbits (γ_0 and γ_f) and the controlled trajectory. The histories of the inputs u_x and u_y are given in Fig. 13. The performance indices are given in Table 3. The total velocity change for the reconfiguration is 3.4173 m/s, and the settling time $T_s = 115,262$ s. The control accelerations are in the ranges of

$$-4.0077 \times 10^{-5} < u_x < 3.7984 \times 10^{-4} \text{ m/s}^2$$

and

$$-2.4945 \times 10^{-4} < u_y < 6.2095 \times 10^{-4} \text{ m/s}^2$$

The initial value of the stabilizing T-periodic solution of the DRE is given by

$$X(0) = \begin{bmatrix} 0.040315 & -0.0021640 & 3.1714 & 16.458 \\ -0.0021640 & 0.00028901 & -0.41878 & -0.85180 \\ 3.1714 & -0.41888 & 612.20 & 1251.5 \\ 16.458 & -0.85180 & 1251.5 & 6728.5 \end{bmatrix}$$

The sizes of the initial and final orbits in Examples 1 and 2 are of the same order as those of an example of the TH equations in [15], in which the initial time to start control action is optimized, and the total velocity change for the reconfiguration is 2.5969 m/s, and the settling time is $T_s = 100,341$ s. The performance indices in Examples 1 and 2 are of the same order, and hence the feedback controller (26) is equally effective both for the TH equations and the nonlinear relative dynamics.

Table 3 Performance indices: example 2

Performance indices	Values
$\|u\|_1$	3.4173 m/s
$\|u\|_2$	2.6875×10^{-2} m/s$^{3/2}$
T_s	115,262 s
$u_x^{\max}$	3.7984×10^{-4} m/s^2
$u_y^{\max}$	6.2095×10^{-4} m/s^2

Table 4 Performance indices: example 3

Performance indices	Values
$\|u_{\text{in}}\|_1$	6.2124×10^{-2} m/s
$\|u_{\text{in}}\|_2$	2.8047×10^{-4} m/s$^{3/2}$
$\|u_z\|_1$	10.821 m/s
$\|u_z\|_2$	5.9816×10^{-2} m/s$^{3/2}$
T_s	167,046 s
$u_x^{\max}$	1.7324×10^{-6} m/s^2
$u_y^{\max}$	8.0799×10^{-6} m/s^2
$u_z^{\max}$	6.4671×10^{-4} m/s^2

Example 3. Noncoplanar Formation. Consider the initial and final orbits given, respectively, by $\gamma_0 = (a_L, 0.731\boldsymbol{i}, 0, 0, 0, 0)$ and $\gamma_f = (a_L, 0.731\boldsymbol{i}, 0, 0, 002, 0)$. The initial orbit is coplanar, and its perifocal reference system is (X_0, Y_0, Z_0). At time $t_0 = 0$, the leader and the follower are on the X_0 axis. The final orbit is the $\phi = 0.002$ rad rotation of the initial orbit γ_0, and the initial position of the virtual satellite at $t_{f0} = t_0 = 0$ is on the $\bar{X}_0$ axis, where $(\bar{X}_0, \bar{Y}_0, \bar{Z}_0)$ is the corresponding perifocal reference system. The initial conditions at $t_0 = 0$ of the follower and the virtual satellite are given by

$$\boldsymbol{x}_0 = [-6.4001 \;\; 0.00000 \;\; 0.00000 \;\; 0.015547 \;\; 0.00000 \;\; 0.00000]$$

$$\boldsymbol{x}_{f0} = [-6.4133 \;\; 0.00000 \;\; 0.00000 \;\; 0.015568 \;\; 13.243 \;\; 0.00000]$$

Thus, the out-of-plane motion is the main motion of the follower. There are two additional penalty parameters in this example, which are set as $q_5 = 1.0 \times 10^{-9}$ and $q_6 = 0$. Figure 14 shows the initial and final orbits and the controlled trajectory. The histories of the inputs are given in Fig. 15. The performance indices are given in Table 4. The total velocity change for the out-of-plane motion is 10.821 m/s and is large compared with those of the in-plane motion in the previous examples. The in-plane motion is negligible in this example, and the total velocity change is 6.2124×10^{-2}. Hence, the total velocity change for the reconfiguration is 10.822 m/s. The settling time is $T_s = 167,046$ s and is large compared with those of the previous examples. The initial value of the stabilizing T-periodic solution of the DRE is given by

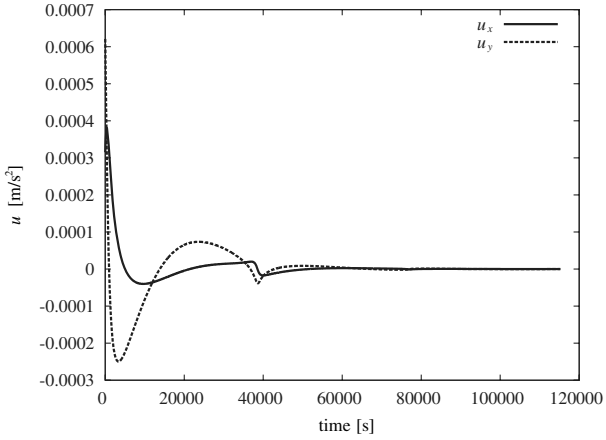

Fig. 13 History of control input: coplanar/general.

$$X(0) = \mathrm{diag}\left\{ \begin{bmatrix} 0.040315 & -0.0021630 & 3.1708 & 16.458 \\ -0.0021629 & 0.00028889 & -0.41876 & -0.85139 \\ 3.1708 & -0.41876 & 612.10 & 1251.3 \\ 16.458 & -0.85139 & 1251.3 & 6728.6 \end{bmatrix}, \begin{bmatrix} 0.000095626 & 0.030171 \\ 0.030171 & 19.977 \end{bmatrix} \right\}$$

V. Conclusions

This paper gives a complete characterization of the initial conditions of all periodic solutions of the nonlinear relative dynamics along an eccentric orbit. An explicit formula for the initial position and velocity is given in terms of the mean motion, semimajor axis, and eccentricity of the leader's inertial orbit; the initial true anomaly and eccentricity of the follower's inertial orbit; and two of the Euler angles of the follower's perifocal reference frame relative to that of the leader. These periodic relative orbits lead to a natural formation problem using the original nonlinear relative dynamics. In this study, feedback controllers of the linear quadratic regulator theory are employed, and as a main performance index, the total velocity change for the formation acquisition or reconfiguration is adopted. By numerical calculations it has been confirmed that the total velocity change for formation acquisition and reconfiguration decreases monotonically as the penalty on control increases. This property is due to the null controllability with vanishing energy of the Tschauner–Hempel system. The settling time, on the other hand, increases as the penalty on control increases. This gives a design method of suboptimal controllers. Numerical simulations using a suboptimal controller have shown that the total velocity change and the settling time for coplanar reconfiguration problems are close to those for the Tschauner–Hempel system given by Shibata and Ichikawa [15]. Moreover, the maxima of the absolute values of control accelerations are very small. Thus, feedback controllers of the linear quadratic regulator theory are equally effective for the new formation acquisition and reconfiguration problems based on the periodic solutions of the nonlinear relative dynamics.

As a future work, the generation of periodic solutions of the nonlinear relative dynamics with additional perturbations is important. It is also useful to express initial conditions of this paper in terms of the orbital elements of the leader and follower.

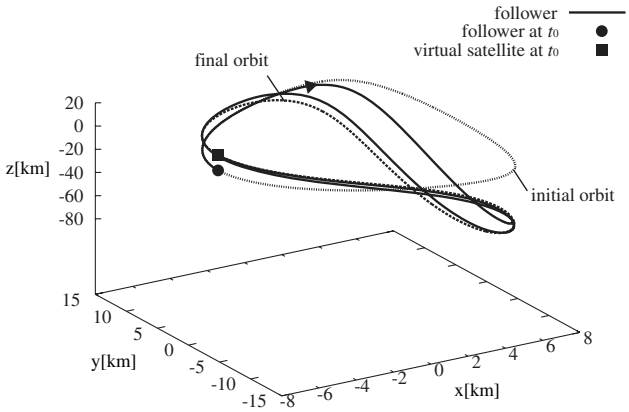

Fig. 14 Controlled trajectory: noncoplanar.

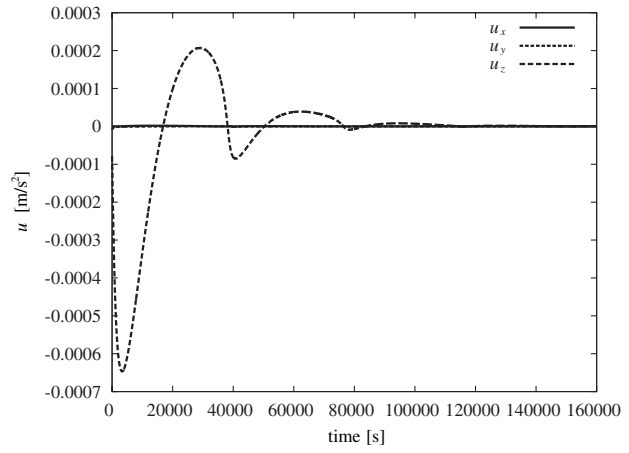

Fig. 15 History of control input: noncoplanar.

Acknowledgments

The authors would like to thank the Associate Editor and the reviewers for their helpful comments on the paper.

References

[1] Clohessy, W. H., and Wiltshire, R. S., "Terminal Guidance System for Satellite Rendezvous," *Journal of Aerospace Science*, Vol. 27, No. 5, 1960, pp. 653–658.

[2] Prussing, J. A., and Conway, B. A., *Orbital Mechanics*, Oxford Univ. Press, New York, 1993, pp. 139–152.

[3] Vallado, D. A., "Fundamentals of Astrodynamics and Applications," 2nd ed., Microcosm Press, El Segundo, CA, and Kluwer Academic, Boston, 2001, pp. 374–399.

[4] Wie, B., *Space Vehicle Dynamics and Control*, AIAA, Reston, VA, 1998, pp. 282–285.

[5] Vassar, R. H., and Sherwood, R. B., "Formationkeeping for a Pair of Satellite in a Circular Orbit," *Journal of Guidance, Control, and Dynamics*, Vol. 8, No. 2, 1985, pp. 235–242. doi:10.2514/3.19965

[6] Leonard, C. L., Hollister, W. M., and Bergmann, E. V., "Orbital Formationkeeping with Differential Drag," *Journal of Guidance, Control, and Dynamics*, Vol. 12, No. 1, 1989, pp. 108–113. doi:10.2514/3.20374

[7] Redding, D. C., Adams, N., and Kubiak, E. T., "Linear-Quadratic Stationkeeping for the STS Orbiter," *Journal of Guidance, Control, and Dynamics*, Vol. 12, No. 2, 1989, pp. 248–255. doi:10.2514/3.20398

[8] Kapila, V., Sparks, A. G., Buffington, J. M., and Yan, Q., "Spacecraft Formation Flying: Dynamics and Control," *Journal of Guidance, Control, and Dynamics*, Vol. 23, No. 3, 2000, pp. 561–564. doi:10.2514/2.4567

[9] Kong, E. M., Miller, D. W., and Sedwick, R. J., "Exploiting Orbital Dynamics for Aperture Synthesis Using Distributed Satellite Systems: Application to a Visible Earth Imager System," *Journal of the Astronautical Sciences*, Vol. 47, Nos. 1–2, 1999, pp. 53–75.

[10] Kang, W., Sparks, A., and Banda, S., "Coordinate Control of Multisatellite Systems," *Journal of Guidance, Control, and Dynamics*, Vol. 24, No. 2, 2001, pp. 360–368. doi:10.2514/2.4720

[11] Campbell, M. E., "Planning Algorithm for Multiple Satellite Clusters," *Journal of Guidance, Control, and Dynamics*, Vol. 26, No. 5, 2003, pp. 770–780. doi:10.2514/2.5111

[12] Schaub, H., "Relative Orbit Geometry Through Classical Orbit Element Differences," *Journal of Guidance, Control, and Dynamics*, Vol. 27, No. 5, 2004, pp. 839–848. doi:10.2514/1.12595

[13] Vaddi, S. S., Alfriend, K. T., Vadali, S. R., and Sengupta, P., "Formation Establishment and Reconfiguration Using Impulsive Control," *Journal of Guidance, Control, and Dynamics*, Vol. 28, No. 2, 2005, pp. 262–268. doi:10.2514/1.6687

[14] Palmer, P., "Optimal Relocation of Satellites Flying Near-Circular-Orbit Formations," *Journal of Guidance, Control, and Dynamics*, Vol. 29, No. 3, 2006, pp. 519–526. doi:10.2514/1.14310

[15] Shibata, M., and Ichikawa, A., "Orbital Rendezvous and Flyaround Based on Null Controllability with Vanishing Energy," *Journal of Guidance, Control, and Dynamics*, Vol. 30, No. 4, July–Aug. 2007, pp. 934–945.
doi:10.2514/1.24171

[16] Ichimura, Y., and Ichikawa, A., "Optimal Impulsive Relative Orbit Transfer Along a Circular Orbit," *Journal of Guidance, Control, and Dynamics*, Vol. 31, No. 4, July–Aug. 2008, pp. 1014–1027.
doi:10.2514/1.32820

[17] Bando, M., and Ichikawa, A., "Periodic Orbits of Nonlinear Relative Dynamics and Satellite Formation," *Journal of Guidance, Control, and Dynamics*, Vol. 32, No. 4, July–Aug. 2009, pp. 1200–1208.
doi:10.2514/1.41438

[18] Carter, T. E., "Optimal Impulsive Space Trajectories Based on Linear Equations," *Journal of Optimization Theory and Applications*, Vol. 70, No. 2, 1991, pp. 277–297.
doi:10.1007/BF00940627

[19] Carter, T. E., and Brient, J., "Fuel-Optimal Rendezvous Problem for Linearized Equations of Motion," *Journal of Guidance, Control, and Dynamics*, Vol. 15, No. 6, 1992, pp. 1411–1416.
doi:10.2514/3.11404

[20] Carter, T. E., and Brient, J., "Linearized Impulsive Rendezvous Problem," *Journal of Optimization Theory and Applications*, Vol. 86, No. 3, 1995, pp. 553–584.
doi:10.1007/BF02192159

[21] Inalhan, G., Tillerson, M., and How, J. P., "Relative Dynamics and Control of Spacecraft Formations in Eccentric Orbits," *Journal of Guidance, Control, and Dynamics*, Vol. 25, No. 1, 2002, pp. 48–59.
doi:10.2514/2.4874

[22] Yamanaka, K., and Ankersen, F., "New State Transition Matrix for Relative Motion on an Arbitrary Elliptical Orbit," *Journal of Guidance, Control, and Dynamics*, Vol. 25, No. 1, 2002, pp. 60–66.
doi:10.2514/2.4875

[23] Sengupta, P., and Vadali, S. R., "Relative Motion and the Geometry of Formations in Keplerian Elliptic Orbits," *Journal of Guidance, Control, and Dynamics*, Vol. 30, No. 4, 2007, pp. 953–964.
doi:10.2514/1.25941

[24] Gurfil, P., "Relative Motion Between Elliptic Orbits: Generalized Boundedness Conditions and Optimal Formationkeeping," *Journal of Guidance, Control, and Dynamics*, Vol. 28, No. 4, 2005, pp. 761–767.
doi:10.2514/1.9439

[25] Sengupta, P., Sharma, R., and Vadali, S. R., "Periodic Relative Motion Near a Keplerian Elliptic Orbit with Nonlinear Differential Gravity," *Journal of Guidance, Control, and Dynamics*, Vol. 29, No. 5, 2006, pp. 1110–1121.
doi:10.2514/1.18344

[26] Ketema, Y., "Optimal Satellite Transfers Using Relative Motion Dynamics," *Journal of Guidance, Control, and Dynamics*, Vol. 32, No. 5, Sept.–Oct. 2009, pp. 1508–1518.
doi:10.2514/1.42847

[27] Priola, E., and Zabczyk, J., "Null Controllability with Vanishing Energy," *SIAM Journal on Control and Optimization*, Vol. 42, 2003, pp. 1013–1032.
doi:10.1137/S0363012902409970

[28] Ichikawa, A., "Null Controllability with Vanishing Energy for Discrete-Time Systems," *Systems and Control Letters*, Vol. 57, No. 1, 2008, pp. 34–38.
doi:10.1016/j.sysconle.2007.06.008

[29] Ichikawa, A., and Katayama, H., "Linear Time-Varying Systems and Sampled-Data Systems," Springer–Verlag, London, 2001, pp. 19–27.